BIOCHEMISTRY
including biophysical chemistry & molecular biology

Article

pubs.acs.org/biochemistry

Crystal Structure of the C-Terminal Globular Domain of Oligosaccharyltransferase from *Archaeoglobus fulgidus* at 1.75 Å Resolution

Shunsuke Matsumoto,[†] Mayumi Igura,[†] James Nyirenda,[†] Masaki Matsumoto,[‡] Satoru Yuzawa,[§] Nobuo Noda,[⊥,#] Fuyuhiko Inagaki,[⊥] and Daisuke Kohda*[,†,∥]

[†]Division of Structural Biology, [‡]Department of Molecular and Cellular Biology, Medical Institute of Bioregulation, [§]Department of Biochemistry, Graduate School of Medical Sciences, and [∥]Research Center for Advanced Immunology, Kyushu University, Maidashi 3-1-1, Higashi-ku, Fukuoka 812-8582, Japan

[⊥]Department of Structural Biology, Graduate School of Pharmaceutical Sciences, Hokkaido University, N-12, W-6 Kita-ku, Sapporo 060-0812, Japan

Supporting Information

ABSTRACT: Protein N-glycosylation occurs in the three domains of life. Oligosaccharyltransferase (OST) transfers glycan to asparagine in the N-glycosylation sequon. The catalytic subunit of OST is called STT3 in eukaryotes, AglB in archaea, and PglB in eubacteria. The genome of a hyperthermophilic archaeon, *Archaeoglobus fulgidus*, encodes three AglB paralogs. Two of them are the shortest AglBs across all domains of life. We determined the crystal structure of the C-terminal globular domain of the smallest AglB to identify the minimal structural unit. The *Archaeoglobus* AglB lacked a β-barrel-like structure, which had been found in other AglB and PglB structures. In agreement, the deletion in a larger *Pyrococcus* AglB confirmed its dispensability for the activity. By contrast, the *Archaeoglobus* AglB contains a kinked helix bearing a conserved motif, called DK/MI motif. The lysine and isoleucine residues in the motif participate in the Ser/Thr recognition in the sequon. The *Archaeoglobus* AglB structure revealed that the kinked helix contained an unexpected insertion. A revised sequence alignment based on this finding identified a variant type of the DK motif with the insertion. A mutagenesis study of the *Archaeoglobus* AglB confirmed the contribution of this particular type of the DK motif to the activity. When taken together with our previous results, this study defined the classification of OST: one group consisting of eukaryotes and most archaea possesses the DK-type Ser/Thr pocket, and the other group consisting of eubacteria and the remaining archaea possesses the MI-type Ser/Thr pocket. This classification provides a useful framework for OST studies.

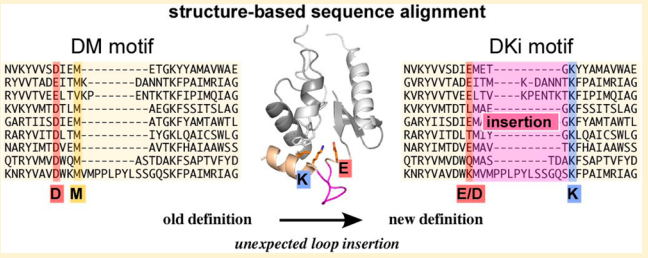

Asparagine-linked glycosylation (N-glycosylation) of proteins is widespread not only in eukaryotes but also in archaea and some eubacteria.[1−4] Oligosaccharyltransferase (OST) creates the oligosaccharide−asparagine bond by transferring a glycan from a lipid-linked oligosaccharide (LLO) to asparagine residues in the N-glycosylation sequon, Asn-X-Ser/Thr (X ≠ Pro).[5−7] OST is a multi-subunit membrane protein complex in higher eukaryotes and a single-subunit membrane protein in lower eukaryotes, archaea, and eubacteria.[1,8−10] The catalytic subunit of the OST enzyme has a common evolutionary origin but is referred to as STT3 (staurosporine and temperature sensitivity 3) in eukaryotes, AglB (archaeal glycosylation B) in archaea, and PglB (protein glycosylation B) in eubacteria. The STT3/AglB/PglB proteins consist of an N-terminal multispan transmembrane region (400−600 residues) and a soluble C-terminal, globular domain (150−500 residues).[11,12] The STT3 proteins share more than 40% sequence identity but exhibit limited sequence identity with the AglB and PglB proteins, typically less than 20%. Thus, a meaningful multiple sequence alignment across the three domains of life was almost impossible, with just one exception. The C-terminal globular domain contains a 5-residue motif, WWDYG, and its strong conservation enables multiple sequence alignment up to 100 residues, using the WWDYG motif as the pivot.[10] As for the sequence alignment of the remaining regions, the three-dimensional structures are required as references.

We previously determined the crystal structures of the C-terminal globular domains of *Pyrococcus furiosus* AglB and *Campylobacter jejuni* PglB.[10,13] These structures facilitated the multiple sequence alignment in the C-terminal globular domain region. Even though they are catalytically inactive, the structural comparison unexpectedly led to the identification of a new, short motif within a characteristic, kinked helix. This kinked

Received: October 10, 2011
Revised: May 3, 2012
Published: May 4, 2012

helix is interesting, since the N-terminal half adopts an exceptionally long (i.e., 6-residue) 3_{10} helical conformation in the *Pyrococcus* and *Campylobacter* structures, while a 3_{10} helix is usually at most 3 residues long. Thus, it is reasonable to assume that the unstable local structure is evolutionarily conserved for a special purpose. In fact, a comprehensive phylogenetic analysis revealed two conserved amino acid motifs within the kinked helix—D*XXKXXX*(M/I) and M*XXIXXX*(I/V/W)—and the two consensus sequences were referred to as DK and MI, respectively.[13] A single genome may encode two or more paralogs. The phylogenetic analysis also revealed that the STT3/AglB/PglB paralogs in one organism contain the same type of motif. All STT3 proteins contain the DK motif, whereas all PglB proteins contain the MI motif. In contrast, the AglB proteins can be divided into three groups, bearing the DK motif, the MI motif, and a third motif. The consensus of the third motif was deduced to be D*XXMXXXK*, and it was tentatively named the DM motif, but without a corresponding structure, the consensus remained ambiguous.

The full-length *Campylobacter lari* PglB structure was recently determined at 3.4 Å resolution.[14] Reflecting the high sequence identity, 52%, the C-terminal globular domains of the two *Campylobacter* PglB proteins superimposed well (Figure S1 of Supporting Information). The reported *C. lari* PglB structure is a complex with an acceptor peptide. Thus, the binding of the peptide substrate does not induce large conformational changes in the C-terminal globular domain of PglB. The crystal structure of the full-length *C. lari* PglB revealed several catalytically important acidic residues on the extracellular loops in the N-terminal transmembrane region and provided insight into the catalytic mechanism. The carboxylate groups of these acidic residues coordinate a divalent metal ion. Two of them also coordinate the amide group of the Asn side chain in the sequon. This simultaneous hydrogen bonding was proposed as an activation mechanism of the amide, which is otherwise a poor nucleophile. Contrary to the previous proposals,[15,16] the Asn-X-Thr portion of the acceptor peptide adopted an extended conformation in the bound state, which suggests the indirect involvement of the hydroxyl group of the +2 Ser/Thr residue in the catalytic reaction. Instead, the *C. lari* PglB structure indicated that the WWD part of the WWDYG motif, and the Ile residue in the MI motif formed a small pocket that recognized the hydroxyl group and the methyl group of the +2 Thr residue in the sequon, respectively. Thus, the +2 Ser/Thr residue, especially its hydroxyl group, in the N-glycosylation sequon is used to guide the side-chain carboxamide group of the Asn residue into the catalytic site.

Here, we determined the crystal structure of the C-terminal globular domain of *Archaeoglobus fulgidus* AglB-S1 at 1.75 Å resolution. The genome of the hyperthermophilic archaeon, *Archaeoglobus fulgidus,* encodes three AglB paralogs. One long AglB (AF_0380) consists of 868 residues and is called *Af*AglB-L, and the other two short AglBs (AF_0329 and AF_0040) consist of 591 and 593 residues and are called *Af*AglB-S1 and *Af*AglB-S2, respectively. We selected *Archaeoglobus fulgidus* as a protein source to assess the tentative DM motif. *Archaeoglobus fulgidus* belongs to the class Archaeoglobi. This archaeal class, along with the other archaeal classes, Halobacteria and Methanomicrobia, was previously proposed to possess the DM motif.[13] In addition, *Af*AglB-S1 is the shortest STT3/AglB/PglB, among the three domains of life (Figure S2 of Supporting Information). We expected to elucidate a common structural unit among the OST enzymes. In the present study, we found that the C-terminal globular domain of *Af*AglB-S1 lacked the β-barrel-like structure found in other AglB/PglB structures and contained an unexpected insertion loop in the kinked helix. Consideration of the inserted sequence improved the multiple sequence alignment and redefined the tentative DM motif. We performed mutagenesis studies of *P. furiosus* AglB and *A. fulgidus* AglB to confirm these ideas experimentally. The structural comparison of the three distantly related AglB and PglB proteins provided important insights into the classification of the OST enzymes over the entire phylogenetic tree of life.

MATERIALS AND METHODS

Protein Expression and Purification. The DNA sequence of the C-terminal globular domain of *Archaeoglobus fulgidus* AglB-S1 (*Af*AglB-S1, residues 430−591, AF_0329) was amplified by PCR from genomic DNA, using the primers 5′-tcctctttcagggacccGACCTCACCGAAGACTGGAAAGA-3′ and 5′-ttaattaagcctcgagATTAGCTACCCACAACCTCAAAAA-3′. The genomic DNA (NBRC 100126G) was obtained from the NITE Biological Resource Center (Chiba, Japan). The PCR product was cloned into *Sma*I-*Xho*I digested pET-47b (Novagen), using an In-Fusion Advantage PCR Cloning Kit (Clontech), for expression in *E. coli* cells with an N-terminal His_6 tag. The two primers contained a 15 bp extension (in lower-case characters) complementary to the linearized pET-47b ends. The cysteine residue at position 482 was replaced by alanine, using a QuikChange mutagenesis kit (Stratagene), to prevent intermolecular disulfide bond formation. The expression plasmid was transformed into *E. coli* BL21 Gold (DE3) cells (Stratagene). *E. coli* cells were grown at 310 K in selenomethionine core medium (Wako) supplemented with 50 mg L^{-1} L-selenomethionine (Nacalai Tesque) and 30 mg L^{-1} kanamycin. When the A_{600} reached 0.6, isopropyl-1-thio-β-D-thiogalactopyranoside was added to a final concentration of 0.5 mM. After 4 h induction at 310 K, the cells were harvested by centrifugation. The cell pellets were suspended in TS buffer (50 mM Tris buffer, pH 8.0, 100 mM NaCl) and disrupted by sonication. After centrifugation, the lysate was heat-treated at 70 °C for 5 min. The thermostable recombinant protein remained in the supernatant. After removing the precipitated proteins by centrifugation, the recombinant protein was purified by affinity chromatography on nickel sepharose high performance resin (GE Healthcare), and the N-terminal His tag was removed by 3C protease, leaving a Gly-Pro-Gly extension at the N-terminus. The cleaved protein was further purified by size-exclusion chromatography, using a Superdex75 column (GE Healthcare) in TS buffer, and then by anion exchange chromatography, using a Resource Q column (GE Healthcare) with a linear NaCl gradient in TS buffer.

Crystallization. Initial crystallization screening was performed by the sitting drop vapor diffusion method, using the index crystallization screen (Hampton Research). After optimization, crystals grew from a hanging drop with a 1:1 volume ratio (total volume, 2 μL) of the protein stock solution (20 mg/mL, 20 mM Tris buffer, pH 8.0) and the reservoir solution (0.1 M MES buffer, pH 6.5, 12.5% poly(ethylene glycol) 3350) at 293 K. Crystals were soaked in the reservoir solution containing 20% ethylene glycol for cryoprotection and were cryo-cooled in liquid nitrogen.

Structure Determination. The diffraction data were processed using the program HKL2000 [17] to resolutions of 1.94 Å (data set 1) and 1.75 Å (data set 2). The crystals

Table 1. Data Collection, Phasing, and Refinement Statistics

	data set 1	data set 2
data collection statistics		
beamline	PF BL-5A	SPring8 BL44XU
wavelength (Å)	0.9788	0.9798
oscillation range (deg)	720	360
space group	$P4_12_12$	$P4_12_12$
cell parameters (Å)	a = 47.04, c = 159.65	a = 47.05, c = 159.82
resolution range (Å)	50.0−1.94 (1.97−1.94)	50.0−1.75 (1.78−1.75)
obsd reflections	714 043	512 201
unique reflections	13 903	18 986
completeness (%)	98.6 (99.4)	98.9 (93.9)
$R_{merge}(I)$[a]	0.067 (0.257)	0.062 (0.399)
$I/\sigma(I)$	126.4/21.4	98.6/13.0
phasing statistics		
resolution range (Å)	25.6−1.94	
no. of Se sites	6	
phasing power	2.04	
figure of merit (acentric/centric)	0.470/0.093	
refinement statistics		
resolution range (Å)		50.0−1.75
no. of protein atoms		1301
no. of water molecules		154
R/R_{free}		0.223/0.254
rmsd[b] from ideality bond length (Å)		0.005
angles (deg)		1.12

[a] $R_{merge}(I) = (\sum\sum|I_i - \langle I\rangle|)/\sum\sum I_i$, where I_i is the intensity of the ith observation and $\langle I\rangle$ is the mean intensity. Values in parentheses refer to the outer shell. [b] rmsd = root-mean-square deviation.

contained one protein molecule per asymmetric unit (V_M = 2.3 Å^3 Da^{-1}, calculated solvent content 46.7%). The initial phasing was performed by the single-wavelength anomalous dispersion method, using the peak data of the selenomethionine-labeled protein crystal (data set 1). After identifying six selenium sites, the initial phases were calculated using the automated structure solution system, autoSHARP,[18] with a mean figure of merit value of 0.470/0.093 for acentric/centric reflections. After the phases were improved by density modification using autoSHARP, automated model building was performed using the program ARP/wARP.[19] Further manual rebuilding and crystallographic refinement were performed with the programs COOT [20] and CNS,[21] respectively, using the low remote data (data set 2). Data collection, phasing, and refinement statistics are summarized in Table 1. The atomic coordinates of the SeMet derivative of the C-terminal globular domain of *Archaeoglobus fulgidus* AglB (AF_0329) have been deposited in the Protein Data Bank, with the accession code 3VGP.

The figures were generated with the PyMOL Molecular Graphics System, Version 1.3 (Schrödinger, LLC). Superposition of the two structures was performed by the program GASH (available on the Protein Data Bank Japan Web site).[22] The multiple sequence alignment was performed with the program MAFFT, version 6 (available on the World Wide Web).[23]

Preparation of the *E. coli* Membrane Fractions Containing the Full-Length *Archaeoglobus fulgidus* AglB-S1. The DNA encoding the full-length *Af*AglB-S1 gene (residues 1−591) was amplified from genomic DNA and cloned into the pET-21d(+) vector (Novagen) between the *Bam*HI and *Xho*I sites. The expressed *Af*AglB-S1 has an N-terminal T7 tag and a C-terminal His_6 tag. The AglB mutants were generated using a KOD plus mutagenesis kit (TOYOBO). The AglB protein and its mutants were expressed in *E. coli* C43 (DE3) cells (Lucigen). The procedures for protein expression and preparation were essentially the same as those described for *Pyrococcus furiosus* AglB,[24] with minor modifications as follows: Instead of LB medium, overnight express TB medium (Merck) was used for expression. After His-tag purification, *Af*AglB-S1 was identified as a major band in a Coomassie Brilliant Blue-stained SDS-PAGE gel, but other minor bands still existed (Figure S3 of Supporting Information). Thus, the amount of the *Af*AglB-S1 protein was quantified by Western blotting, with mouse anti-T7 tag antibodies (Merck) and goat anti-mouse IgG antibodies labeled with a fluorescent IR Dye 800CW (LI-COR). The fluorescent images were measured with an Odyssey Infrared Imaging system (LI-COR) and were quantified with the Odyssey software V3.0.

A *Pyrococcus furiosus* full-length AglB mutant that lacks the IS domain (residues 603−678), designated as *Pf*AglBΔIS, was generated by the inverse PCR method.[25] The preparation method of the *E. coli* membrane fractions containing *Pf*AglBΔIS was the same as that for the wild type.[24] The wild-type *Pf*AglB migrated as two bands with smearing between them on SDS-PAGE due to the high thermostability of the *Pf*AglB protein. This was not problematic for protein quantification,[24] but the integration of large areas was necessary. We recently found that TCA (trichloroacetic acid) treatment before SDS-PAGE resulted in one band on SDS-PAGE. Briefly, an equal volume of a 10% (w/v) TCA solution was added to the protein sample, which was kept on ice for 10 min, and then the protein pellet was recovered by centrifugation, washed with cold acetone, and air-dried. The amounts of the *Pf*AglB and *Pf*AglBΔIS proteins were quantified by Western blotting, with mouse anti-His tag antibodies

dx.doi.org/10.1021/bi300076u | *Biochemistry* 2012, 51, 4157−4166

(QIAGEN) and goat anti-mouse IgG antibodies labeled with the fluorescent IR Dye 800CW.

Preparation of Lipid-Linked Oligosaccharide from *Archaeoglobus fulgidus* Cells. The *A. fulgidus* type strain (DSM 4306, NBRC No. 100126) was obtained from the NITE Biological Resource Center (Chiba, Japan). *Archaeoglobus fulgidus* medium was prepared according to the provider's protocol, but sodium carbonate was omitted to avoid precipitation after autoclaving. *A. fulgidus* cells were grown in 1 L culture bottles anaerobically without shaking for 5 days at 80 °C in an oven. Three grams of pelleted cells were obtained from a 10 L culture. *A. fulgidus* LLO was prepared according to the procedure used for *P. furiosus* LLO extraction.[10]

Oligosaccharyltransferase Assay. The OST assay was performed by the PAGE method.[26] The reaction mixture (total 12 μL) for *Af*AglB-S1 contained 30 mM Tris buffer, pH 7.5, 6 mM $MnCl_2$, dried LLO prepared from *A. fulgidus* cells (equivalent to 5 μL), 3 μL of the *E. coli* membrane fraction containing the full-length *Af*AglB-S1 or its mutant, and 1 μL of 0.1 mM substrate peptide solution. The preparation of a set of peptides, TAMRA-Gly-X-X-X-Val-Thr-NH_2, where the X-X-X sequence was varied for testing the N-glycosylation dependency, was reported previously.[10] A fluorescent dye, TAMRA, and an amide group were attached at the N-terminal amino group and the C-terminal carboxyl group, respectively. The substrate peptide used for the specific OST activity assay was NH_2−Ala-Ala-Tyr-Asn-Val-Thr-Lys-Arg-(Lys-TAMRA), in which the N-glycosylation sequon is underlined. The TAMRA dye was attached to the side-chain amino group of the C-terminal Lys residue. The reaction was performed for 2 h at 60 °C. We performed a time course of the reaction and confirmed the linearity of the reaction even after 4 h (Figure S4 of Supporting Information, an overall image of the SDS-PAGE analysis is provided). The reaction was stopped by the addition of 2.4 μL of 5 × SDS sample buffer. The reaction mixtures were separated by Tris-Glycine SDS-PAGE (gradient gel 15−25%). The fluorescence images of the SDS-PAGE gels were recorded with an LAS-3000 multicolor image analyzer (Fuji Photo Film). It was unnecessary to detach the glass plates from the gel. The pixel intensity of the SDS-PAGE bands was quantified and integrated, was corrected by subtracting the background using the Image Gauge software (Fuji Photo Film), and was converted to the molar amount using the published calibration curve.[26] The quantitative performance of the specific OST activity measurement was carefully assessed as in the previous reports, using *Pf*AglB.[24,27] The specific activity (S) was calculated by using the equation $S = A/P$, where A is the mean OST activity and P is the mean amount of protein. The standard deviation (σ_S) of the specific activity was calculated by using the propagation of error equation, $(\sigma_S/S)^2 = (\sigma_A/A)^2 + (\sigma_P/P)^2$.

The assay for *Pf*AglB was performed in a similar way to the *Af*AglB-S1 assay. The reaction mixture contained LLO prepared from *Pyrococcus furiosus* cells and a substrate peptide, TAMRA-Ala-Pro-Tyr-Asn-Val-Thr-Lys-Arg, which was optimized by peptide library experiments.[27] The reaction was performed for 1 h at 65 °C.[24]

Electrospray Ionization Mass Spectrometry Analysis. The reaction mixture of the OST assay was separated using reverse-phase C18 HPLC chromatography in 0.1% trifluoroacetic acid and acetonitrile. The reaction product was collected, dried in a SpeedVac, and dissolved in 0.1% formic acid and 50% methanol. TripleTOF 5600 mass spectrometer (ABSciex) was used for direct-infusion electrospray ionization (ESI) analysis at a flow rate of 1.0 μL/min. The triply charged precursor ion (m/z 864.3861) was selected and subjected to MS/MS analysis with collision energy 30.

RESULTS AND DISCUSSION

Overall Structure of the C-Terminal Globular Domain of *Archaeoglobus fulgidus* AglB-S1. Two of the three *A. fulgidus* AglB paralogous proteins are the smallest catalytic subunits of OST among the three domains of life (Figure S2 of Supporting Information). We designated them as *Af*AglB-S1 and *Af*AglB-S2. The primary sequence of the *Af*AglB-S1 protein consists of the N-terminal transmembrane region (429 residues) and the C-terminal globular domain (162 residues). We determined the crystal structure of the C-terminal globular domain of *Af*AglB-S1 at 1.75 Å resolution (Figure 1 and Table 1). The overall structure is compact and is regarded as one structural domain. It consists of mainly α-helices and contains one three-stranded antiparallel β-sheet.

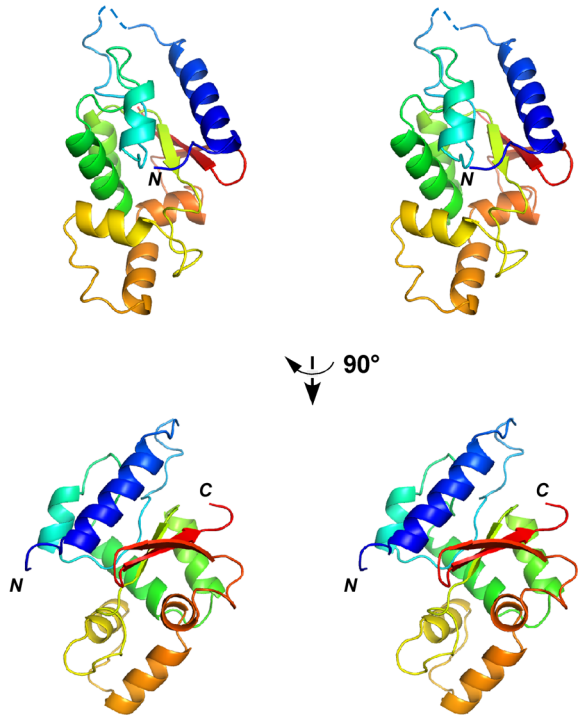

Figure 1. Crystal structure of the C-terminal globular domain of *Archaeoglobus fulgidus* AglB-S1. Stereo views are colored in a blue-red rainbow gradient from the N- to C-terminus. Dashed lines indicate the Leu452 residue, which was not included in the final model due to the incomplete electron density.

Comparison of the AfAglB-S1 Structure with Previously Determined AglB and PglB Structures. We previously reported two crystal structures of the C-terminal globular domains: one structure of archaeal origin, *Pyrococcus furiosus* AglB (*Pf*AglB),[10] and the other of eubacterial origin, *Campylobacter jejuni* PglB (*Cj*PglB).[13] The C-terminal globular domain of *Pf*AglB consists of four structural units, whereas that of *Cj*PglB has two structural units (Figure 2). The common structural unit among the three structures is called CC (central core, in blue). The three CC units share a high level of structural similarity, despite their low sequence identity (about 20%). The root-mean-square deviation of the structural

dx.doi.org/10.1021/bi300076u | *Biochemistry* 2012, 51, 4157−4166

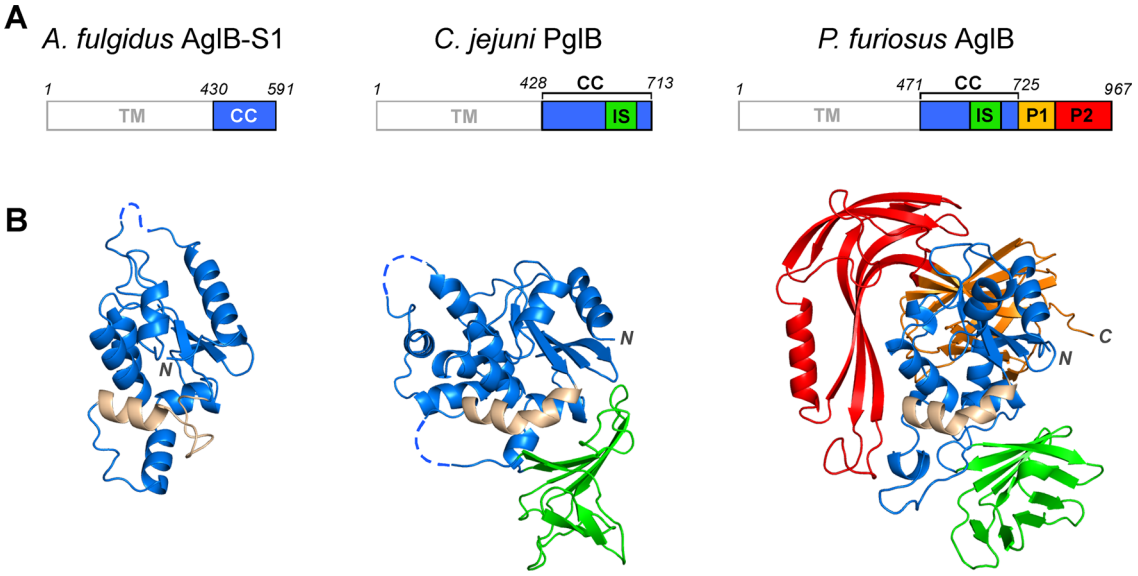

Figure 2. Comparison of the structures of *Archaeoglobus fulgidus* AglB-S1, *Campylobacter jejuni* PglB, and *Pyrococcus furiosus* AglB. (A) Domain organization of the three AglB/PglB proteins. TM, transmembrane; CC, central core; IS, insertion; P1, peripheral 1; P2, peripheral 2. The TM region not included in the structure determination is outlined in gray. (B) Overall structures of the C-terminal globular domains. The CC is colored blue, IS is green, P1 is orange, and P2 is red. The characteristic kinked helix is highlighted in light brown.

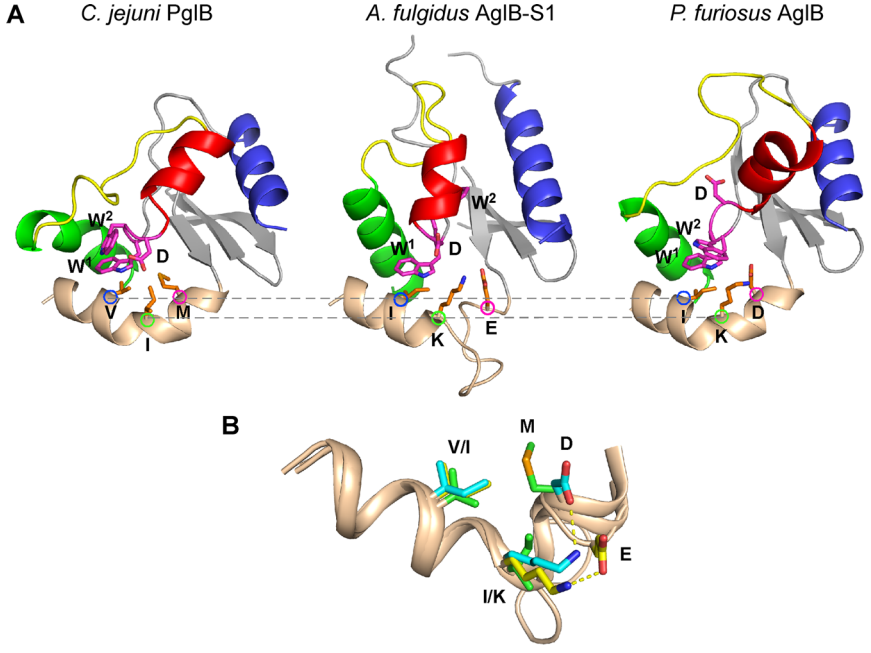

Figure 3. Close-up views of the common local structures among the three structures. (A) The side chains of the WWD part of the WWDYG motif are labeled and colored magenta. The α-helix and loop, which show highly conformational variation in the three structures, are colored red and yellow, respectively. The kinked helix is colored light brown, and the side chains of the three signature residues constituting the DK/MI motif are colored orange. Horizontal dashed lines indicate the correspondence in the positions of the signature residues of the DK/MI motif on the kinked helix. (B) Superimposition of the three kinked helices, with the side chains of the three signature residues of the DK/MI motif. The 10 residues on the C-terminal side of the kinked site were used for superposition. The side chains are colored green, yellow, and cyan for *Cj*PglB, *Af*AglB-S1, and *Pf*AglB, respectively. Yellow dotted lines indicate the formation of a salt bridge. The distances are 2.9 Å for the Glu-Lys pair in *Af*AglB-S1 and 3.3 Å for the Asp-Lys pair in *Pf*AglB.

superposition of the CC units is 2.3 Å between *Af*AglB-S1 and *Pf*AglB over 126 aligned Cα atoms and 2.4 Å between *Af*AglB-S1 and *Cj*PglB over 109 aligned Cα atoms. *Pf*AglB and *Cj*PglB contain a β-barrel-like structure, which is called IS (insertion, in green), because this structural unit seems to have been inserted in the CC structure. The large *Pf*AglB contains two more structural units, called P1 (peripheral 1, in orange) and P2 (peripheral 2, in red). The P1 and P2 units are β-sheet-rich and encircle the CC unit.

Conserved Motifs on the Kinked Helix. We focused our attention on the conserved sequence motifs in the CC unit. All STT3/AglB/PglB proteins contain a highly conserved 5-residue motif, WWDYG, in the CC unit. The first three residues, WWD, form the +2 Ser/Thr-recognizing pocket. There is a

dx.doi.org/10.1021/bi300076u | *Biochemistry* 2012, 51, 4157−4166

characteristic, kinked helix close to the WWDYG motif in the three structures (Figure 2, in light brown). The kinked helices contain a conserved amino acid motif, the DK motif in *Pf*AglB, and the MI motif in *Cj*PglB. The consensus sequence is D*XXKXXX*(M/I) or M*XXIXXX*(I/V/W), deduced from the previous comprehensive phylogenetic analysis.[13] In spite of the vastly different chemical natures of the side chains (D vs M and K vs I), the three signature residues in the two motifs occupy identical spatial positions (Figure 3A). The *Af*AglB-S1 structure revealed that extra amino acid residues were unexpectedly inserted at the kinked site. A visual inspection indicated that the three signature amino acid residues defining the kinked-helix motif are Glu, Lys, and Ile for *Af*AglB-S1. The spatial positions of the second Lys and third Ile residues are identical among the three structures, but that of the first Glu slightly deviated from the canonical position, probably due to the deformation of the N-terminal part from the 3_{10} conformation (Figure 3B). Note that the residue preceding the Glu residue is Asp in the *Af*AglB-S1 sequence, and without reference to the structures, the correct choice of the first signature residue among the two successive acidic residues would be impossible. Considering the insertion, we revised the multiple sequence alignment within and the near the kinked helix region (Figure 4). Thus, the

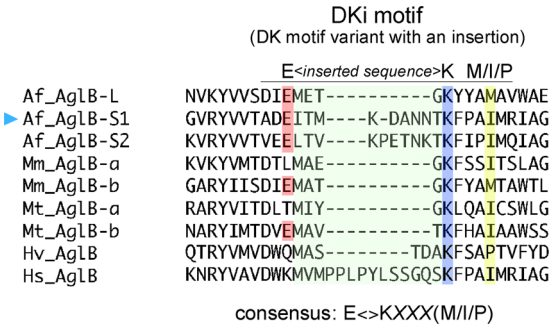

Figure 4. Multiple sequence alignment for redefinition of the variant of the DK motif. This variant DK motif is referred to as DKi, for convenience. Alignment was performed with the program MAFFT. The AglB sequences belonging to the classes Halobacteria, Archaeoglobi, and Methanomicrobia were used: Af_AglB-L (029867_ARCFU), Af_AglB-S1 (029918_ARCFU), Af_AglB-S2 (030195_ARCFU), Mm_AglB-a (Q8PUW8_METMA), Mm_AglB-b (Q8PZ47_METMA), Mt_AglB-a (A0B8C2_METTP), Mt_AglB-b (A0B996_METTP), Hv_AglB (A9JPF0_HALVO), and Hs_AglB (Q9HQP2_HALSA). The blue arrowhead marks the sequence of *A. fulgidus* AglB-S1.

previously proposed consensus, D*XXMXXX*K, must be changed to E⟨⟩K*XXX*(M/I/P), where ⟨⟩ denotes the inserted 9-residue sequence. This revision suggests that the third motif can be regarded as a variant of the DK motif with an inserted sequence. The conserved Met in the previous definition is located on the inserted loop structure and contributes to the formation of a hydrophobic core (Figure S5 of Supporting Information).

Initially, the DK/MI motif was assumed to be a catalytic motif, but the crystal structure of *C. lari* PglB revealed that the second signature residue, Ile, of the MI motif provided a hydrophobic surface for the recognition of the methyl group of Thr, concertedly with the WWDYG motif.[14] By analogy, we suggest that the alkyl portion of the Lys side chain in the DK motif also contributes to the formation of the +2 Ser/Thr-recognition pocket in AglBs and STT3s.

Conformational Variation of the WWDYG Motif. Considerable differences exist between the conformation of the WWDYG motif segment and the following helix and loop in the *Pf*AglB and *Cj*PglB structures (Figure 3A, in magenta, red, and yellow). Part of the WWDYG motif in *Pf*AglB adopted a rare left-handed helical conformation, which was stabilized by the crystal contact effects.[10] The corresponding part formed a typical right-handed helix in *Cj*PglB. Interestingly, the conformation of the WWDYG motif in *Af*AglB-S1 adopts an extended conformation and is thus quite different from those in the other two structures, Although the first Trp residue of the WWDYG motif occupies the equivalent position with the same side-chain orientations among the three structures, the side-chain orientations of the second Trp and the Asp residues are completely different from one another. The WWD part of the WWDYG motif in *Cj*PglB adopts a conformation that is suitable to form the +2 Ser/Thr pocket, but the corresponding parts of *Pf*AglB and *Af*AglB-S1 are distorted in the crystals, probably due to the crystal packing effect. The conformational plasticity seen among the crystal structures suggests the intrinsic flexibility of the C-terminal globular domain in solution, although it is difficult to discuss its biological significance at this point.

Oligosaccharyltransferase Assay for AfAglB-S1. To test the involvement of the DK motif in the enzymatic activity, we developed an *in vitro* oligosaccharyltransferase assay for *Af*AglB-S1. The full-length *A. fulgidus* AglB-S1 protein, with an N-terminal T7 tag and a C-terminal His tag, was expressed in *E. coli* membrane fractions and was partially purified with Ni-affinity resin after solubilization in the presence of 1% *n*-dodecyl-*β*-D-maltoside. The protein amount was quantified by Western blotting, using anti-T7 tag antibodies. Separately, LLO was prepared from cultured *A. fulgidus* cells by chloroform/methanol/water extraction. After mixing the enzyme and *Af*LLO with a fluorescently labeled peptide, the products were separated from the substrate peptides by SDS-PAGE. First, we examined the requirement for the canonical N-glycosylation consensus sequence. Figure 5A shows the results of the OST assay in the presence and absence of *Af*LLO, as an oligosaccharide donor. A single product band was observed when the peptide substrate contained the Asn-X-Thr or Asn-X-Ser sequence, only in the presence of *Af*LLO (lanes 1, 2, and 7). The noncognate LLO prepared from *P. furiosus* cells (*Pf*LLO) did not serve as an oligosaccharide donor (lane 8), indicating the strict specificity for the oligosaccharide moiety. We found that *Pf*AglB also could not use *Af*LLO (data not shown). The Asn-X-Thr sequence was a better substrate than the Asn-X-Ser sequence, as observed in the OST assay of *Pf*AglB using peptide libraries[27] and in the statistical analyses of experimentally verified eukaryotic N-glycosylation sites.[5,28] The replacement of the first residue, Asn, with Gln (lane 3) and that of the third residue, Thr/Ser, with Ala (lane 4) resulted in the disappearance of the product bands. The replacement of the second residue, Ser, with Pro (lanes 5 and 6) also completely blocked the product formation. Thus, the amino acid requirement is fully consistent with the eukaryotic N-glycosylation consensus.

A problem of the present assay is a very low turnover number of the reaction. This is probably due to the use of the detergent solubilized enzyme and LLO. A rough estimate showed 1 mol product/h/mol *Af*AglB-S1 and 0.1% conversion of the peptide input, even after the optimization of the assay conditions. For example, in the original assay method,[26] a fluorescent dye,

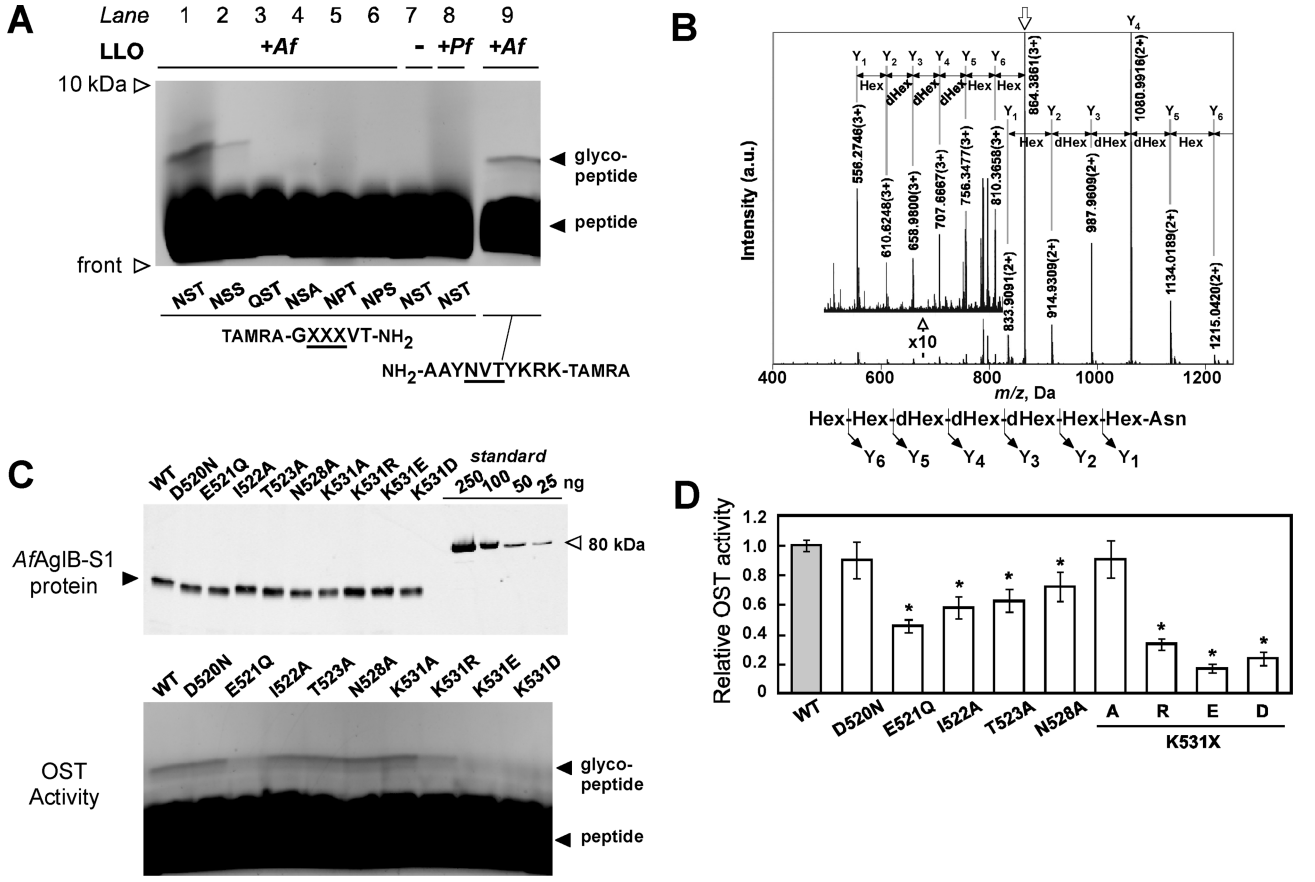

Figure 5. Effects of amino acid substitutions on the OST activity of *Archaeoglobus fulgidus* AglB-S1. (A) Effects of the amino acid substitutions in the N-glycosylation sequon on the OST reaction. The reaction mixtures were subjected to SDS-PAGE, and the fluorescence of the TAMRA dye attached to the peptide was detected at 575 nm. The positions of the MW marker and the tracking dye front are indicated. (B) MS/MS analysis of the reaction product. ESI-MS/MS spectrum of the precursor ion with m/z 864.3861 is shown. The expected m/z was observed within 0.01 Da. The fragment ions originating from the sequential loss of monosaccharide residues are labeled in the spectrum. There are two distinct mass ladders corresponding to the $[M + 3H]^{3+}$ and $[M + 2H]^{2+}$ ions, marked with 2+ and 3+, respectively. The inferred *A. fulgidus* N-glycan structure produced by the recombinant *Af*AglB-S1 is shown with its fragmentation pattern. (C) Upper panel: Western blot image of the wild type (WT) and the point mutants of *Af*AglB-S1, for quantitative measurement of the protein amount. The fluorescence of the secondary antibodies was detected at 800 nm. The amount of an 80 kDa T7-tagged protein is indicated, as an internal protein standard. About 20−40 ng of the *Af*AglB-S1 protein was used per reaction. Lower panel: SDS-PAGE image for the determination of the OST activity. About 20−100 fmol of glycopeptide was formed per reaction. (D) Relative specific *Af*AglB-S1 activity. The specific OST activity of the wild-type protein was defined as 1. The error bars represent the mean ± SD calculated from three independent protein quantifications and three independent OST assays. Data were compared to the wild type by an unpaired two-tailed t-test, assuming unequal variance. $^*P < 0.01$.

TAMRA, was attached at the N-terminus, but the glycopeptide bands in the assay were somewhat blurred (lane 1). We found that the peptide substrate bearing the TAMRA dye at the C-terminus produced a shaper band (lane 9), and therefore, we used this peptide in subsequent experiments. The use of lipid bilayers and coupling with ribosomal protein synthesis will be a key for achieving high turnover numbers of the OST reaction in the future.

We used reverse-phase HPLC chromatography to purify the reaction product by monitoring the fluorescence of the TAMRA dye. The product peptide was eluted as a single new peak, faster than the substrate peptide. The analysis by electrospray ionization mass spectrometry (ESI-MS) showed a triply charged ion as a main peak at m/z 864.3861. The MS/MS analysis of this ion provided a fragmentation series resulting from the sequential loss of two hexoses (Hex, 162.053 Da), three deoxyhexoses (dHex, 146.058 Da), and one Hex (Figure 5B). The smallest fragment ion peak at m/z 556.2746 corresponds to the peptide bearing one Hex residue. Thus, the precursor $[M + 3H]^{3+}$ ion peak at m/z 864.3861, corresponding to monoisotopic mass of 2590.1365 Da, is in excellent agreement with calculated mass of the glycopeptide containing a single oligosaccharide chain comprising four Hex and three dHex (2590.1361 Da). The distinct mass ladders with relatively uniform peak intensities suggest an unbranched heptasaccharide glycan (Figure 5B), but we need further investigation for the precise chemical structure. The Archaeoglobus N-glycan structure is relatively simple among the three domains of life.[29] In particular, the first monosaccharide residue that directly linked to the asparagine residue is a hexose. This is rare because the first monosaccharide moiety of most of the N-glycans contains a N-acetyl group at the C2 position, except for N-glycans from archaeal *Haloferax volcanii* and *Halobacterium salinarum*.[30] Finally, we confirmed that the reaction product purified by HPLC had the same mobility in the SDS-PAGE gels as the product band in the reaction mixture (data not shown). When taken together, the OST assay properly detected and quantified the production of the N-glycosylation of the

dx.doi.org/10.1021/bi300076u | *Biochemistry* 2012, 51, 4157−4166

consensus sequence in the fluorescently labeled peptide by the recombinant *Af*AglB-S1 in the presence of crude LLO from *A. fulgidus* cells.

Mutagenesis Study of the DK Motif of *Archaeoglobus fulgidus* AglB-S1. The protein expression and enzymatic activities of the *Af*AglB-S1 mutants are summarized in Figure 5C. The positions of the mutated residues are shown on the three-dimensional structure in Figure S6 of the Supporting Information. We constructed ten alanine-substituted *Af*AglB-S1 mutants, but six mutants, T518A, D520A, E521A, M524A, D526A, and I535A, were not detected in *E. coli* membrane fractions by Western blotting with anti-His tag antibodies. No degradation products were detected in the membrane fractions, either. These nonproductive mutations include the conserved Met at position 524 in the previous definition of the DM motif and the first and third signature residues of the DK motif. To verify the first signature residue of the DK motif, we constructed two more conservative mutations, D520N and E521Q, which were successfully expressed in the *E. coli* membrane fractions. The D520N mutation showed minimal effects, but the E521Q mutation had inhibitory effects on the OST activity (Figure 5D). This result indicated that E521 was the first signature residue of the DK motif, confirming the conclusion from the visual inspection of the superimposed structures (Figure 3B). At the K position in the DK motif, the K531A mutation slightly reduced the specific activity, but the inhibitory effect was not statistically significant. To characterize the role of the DK motif further, we substituted the Lys residue with Arg, Glu, and Asp at position 531 (Figure 5C,D). These mutations reduced the *Af*AglB-S1 activity substantially. The tendency for decreases in the specific activity arising from differences in the amino acids was very similar to the corresponding mutations of the DK motif in *Pf*AglB.[24] These mutagenesis studies confirmed the validity of the definition of the DK motif on the kinked helix of *Af*AglB-S1.

There is a difference from the previously identified DK/MI motif. The N-terminal part of the kinked helix in *Af*AglB-S1 retains a helical character but deviates from the expected 3_{10} conformation. This conformational difference may have some connection to the unique feature of the *Af*AglB-S1 structure: it lacks the IS structural unit and, instead, contains the inserted sequence at the kinked site. The alanine mutations in the inserted sequences resulted in either reduced activity (I522A, T523A, N528A) or loss of the protein production (M524A, D526A). This finding implies that the inserted sequences found in some Archaeal classes (Figure 4) are necessary for the structural integrity of the Ser/Thr pocket in these AglB proteins.

Effect of the Deletion of the IS Structural Unit of *Pyrococcus furiosus* AglB on the Activity. The β-barrel-like IS units in *Pf*AglB and *Cj*PglB are very interesting at first glance and appear to be structurally or functionally important (Figure 2). To test the role of the IS unit, we constructed a *Pf*AglB mutant lacking the IS unit and expressed it in *E. coli* membrane fractions (Figure 6A). The protein yield of the mutant was the same as that of the wild type (Figure 6B). The specific OST activity was virtually the same, confirming that the IS unit is dispensable for the OST activity (Figure 6C). Note that the present assay used detergent-solubilized *Pf*AglB and a short peptide as an acceptor substrate. It is possible that the IS unit is necessary for structural integrity in plasma membranes in situ or for higher levels of functions, e.g., efficiency or regulation when coupled with ribosomal protein translation. The same

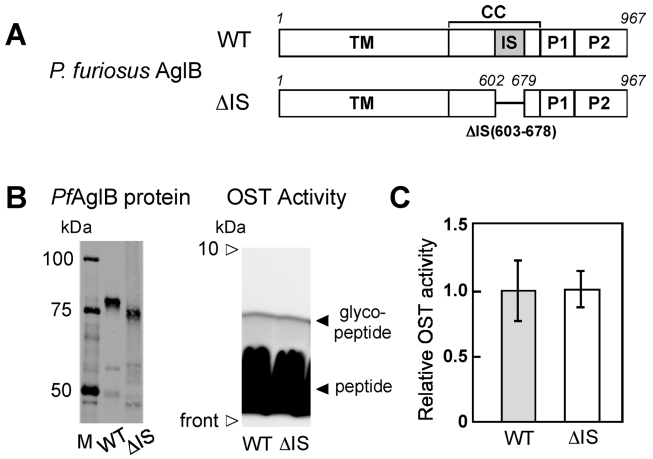

Figure 6. Effect of the deletion of the β-barrel-like IS unit on the OST activity of *Pyrococcus furiosus* AglB. (A) Schematic representation of the construction of the deletion mutant of the IS unit (residues 603–678) of *P. furiosus* AglB. (B) Left panel: Western blot image of the wild type (WT) and the IS-deleted mutant (ΔIS), for quantitative measurement of the protein amount. The fluorescence of the secondary antibodies was detected at 800 nm. The amounts of the His-tagged protein standards (6xHis Protein Ladder, QIAGEN) are 150 ng (100 kDa), 120 ng (75 kDa), and 100 ng (50 kDa). About 30–40 ng of the *Pf*AglB protein were used per reaction. Right panel: SDS-PAGE image for the determination of the OST activity. The fluorescence of the TAMRA dye attached to the N-terminus of the peptide was detected at 575 nm. The positions of the MW marker and the tracking dye front are indicated. Each reaction produced about 200 fmol glycopeptide. (C) Relative specific *Pf*AglB activity. The specific OST activity of the wild-type AglB was defined as 1. The error bars represent the mean ± SD, calculated from three independent protein quantifications and three independent OST assays.

discussion also holds for the P1 and P2 units in *Pf*AglB. It would be quite interesting to determine whether the STT3 protein, as the catalytic subunit in the eukaryotic multisubunit OST complex, possesses the IS unit or other novel structural units, but the limited sequence similarity prevents such a prediction. In this sense, the structures of the STT3 proteins are still required.

■ CONCLUSION

In this study, we reported the third crystal structure of the C-terminal globular domain of the catalytic subunit of oligosaccharyltransferase. The *Archaeoglobus fulgidus* AglB-S1 structure revealed that its C-terminal domain is the minimal architecture in the C-terminal globular region of the catalytic subunit of the OST enzymes, considering the fact that it is the smallest among all of the OSTs. Because of the low sequence homology, a comparative structural biology approach is required to obtain a meaningful multiple sequence alignment. We solved the problem of the alignment within the kinked helix region in the C-terminal globular domain by considering the unexpected inserted sequence within the kinked helix in the *Af*AglB-S1 structure. The improved alignment led to the redefinition of the consensus sequence within the kinked helix.

The OST enzymes over the entire phylogenetic tree of life are now classified into two types: OSTs with the DK motif, including eukaryotes and most archaea, and OSTs with the MI motif, including eubacteria and the remaining archaea (Figure S7 of Supporting Information). A subset of the major group of archaea has a variant DK motif, which is interrupted by an extra

dx.doi.org/10.1021/bi300076u | *Biochemistry* 2012, 51, 4157–4166

sequence of 4−14 residues (Figure 4). All AglBs belonging to the archaeal classes, Archaeoglobi, Halobacteria, and Methanomicrobia, contain the variant of the DK motif. The variant motif may be called DKi (DK motif with an insertion) for convenience. This classification of OST based on the DK/MI motif is not trivial, since the DK/MI motif contributes to the formation of the +2 Ser/Thr recognition pocket, which specifies the positioning of the acceptor asparagine residue in the catalytic site. The Ser/Thr pocket is composed of the invariable WWD part of the WWD(Y/W/F/N)G motif and the second signature residue of the DK/MI motif. The properties of the Ser/Thr pocket are thus dependent on the Lys or Ile residue of the DK/MI motif. The classification of the catalytic subunit of the OST enzymes established in this study will provide a useful framework toward understanding the molecular mechanisms of N-glycosylation in future studies.

■ ASSOCIATED CONTENT

Supporting Information

Seven figures showing the structural comparison between *Campylobacter jejuni* PglB and the *Campylobacter lari* PglB, the distribution of the residue numbers of the STT3/AglB/PglB proteins, the purity of the full-length recombinant *Af*AglB-S1 protein after His-tag purification, the linearity of the time course of the *Af*AglB-S1 assay, the hydrophobic core in the *Af*AglB-S1 structure, the mapping of mutated residues on the three-dimensional structure of *Af*AglB-S1, and a revised version of the multiple sequence alignment of the STT3/AglB/PglB proteins. This material is available free of charge via the Internet at http://pubs.acs.org.

■ AUTHOR INFORMATION

Corresponding Author

*Phone: + 81-92-642-6968. Fax: + 81-92-642-6764. E-mail: kohda@bioreg.kyushu-u.ac.jp.

Present Address

[#]Institute of Microbial Chemistry, Kamiosaki 3-14-23, Shinagawa-ku, Tokyo 141-0021, Japan.

Funding

This work was supported by a Grant-in-Aid for Scientific Research on Innovative Areas 21121003, the Targeted Proteins Research Program (TPRP) from the Ministry of Education, Culture, Sports, Science and Technology (MEXT) of Japan, and Research Grant 090036 from the Mizutani Foundation for Glycoscience to D.K.

Notes

The authors declare no competing financial interest.

■ ACKNOWLEDGMENTS

We thank Ms. Yuki Matsuzaki (Laboratory for Technical Support, Medical Institute of Bioregulation, Kyushu University) for DNA sequencing. We also thank the staffs at beamline BL-5A of Photon Factory (Tsukuba, Japan) and at beamline BL-44XU of SPring-8 (Harima, Japan). The experiments at the Photon Factory were approved by the High Energy Accelerator Research Organization (KEK), as proposals 2009G208 and 2011G020. The experiments at SPring-8 were performed under the Cooperative Research Program of Institute for Protein Research, Osaka University, as proposals 2011A1904, 2011A6619, and 2011B6619.

■ ABBREVIATIONS

AfAglB, *Archaeoglobus fulgidus* AglB; Agl, archaeal glycosylation; CBB, Coomassie Brilliant Blue; CC, central core; CjPglB, *Campylobacter jejuni* PglB; ESI-MS, electrospray ionization mass spectrometry; IS, insertion; LLO, lipid-linked oligosaccharide; MES, 4-morpholineethanesulfonic acid; OST, oligosaccharyltransferase; PfAglB, *Pyrococcus furiosus* AglB; Pgl, protein glycosylation; STT, staurosporine and temperature sensitivity; TAMRA, carboxytetramethylrhodamine; Tris, tris(hydroxymethyl)aminomethane; TCA, trichloroacetic acid.

■ REFERENCES

(1) Knauer, R., and Lehle, L. (1999) The oligosaccharyltransferase complex from yeast. *Biochim. Biophys. Acta 1426*, 259−273.

(2) Burda, P., and Aebi, M. (1999) The dolichol pathway of N-linked glycosylation. *Biochim. Biophys. Acta 1426*, 239−257.

(3) Yan, A., and Lennarz, W. J. (2005) Unraveling the mechanism of protein N-glycosylation. *J. Biol. Chem. 280*, 3121−3124.

(4) Abu-Qarn, M., Eichler, J., and Sharon, N. (2008) Not just for Eukarya anymore: protein glycosylation in Bacteria and Archaea. *Curr. Opin. Struct. Biol. 18*, 544−550.

(5) Petrescu, A. J., Milac, A. L., Petrescu, S. M., Dwek, R. A., and Wormald, M. R. (2004) Statistical analysis of the protein environment of N-glycosylation sites: implications for occupancy, structure, and folding. *Glycobiology 14*, 103−114.

(6) Nita-Lazar, M., Wacker, M., Schegg, B., Amber, S., and Aebi, M. (2005) The N-X-S/T consensus sequence is required but not sufficient for bacterial N-linked protein glycosylation. *Glycobiology 15*, 361−367.

(7) Apweiler, R., Hermjakob, H., and Sharon, N. (1999) On the frequency of protein glycosylation, as deduced from analysis of the SWISS-PROT database. *Biochim. Biophys. Acta 1473*, 4−8.

(8) Feldman, M. F., Wacker, M., Hernandez, M., Hitchen, P. G., Marolda, C. L., Kowarik, M., Morris, H. R., Dell, A., Valvano, M. A., and Aebi, M. (2005) Engineering N-linked protein glycosylation with diverse O antigen lipopolysaccharide structures in Escherichia coli. *Proc. Natl. Acad. Sci. U. S. A. 102*, 3016−3021.

(9) Kelleher, D. J., and Gilmore, R. (2006) An evolving view of the eukaryotic oligosaccharyltransferase. *Glycobiology 16*, 47R−62R.

(10) Igura, M., Maita, N., Kamishikiryo, J., Yamada, M., Obita, T., Maenaka, K., and Kohda, D. (2008) Structure-guided identification of a new catalytic motif of oligosaccharyltransferase. *EMBO J. 27*, 234−243.

(11) Kim, H., von Heijne, G., and Nilsson, I. (2005) Membrane topology of the STT3 subunit of the oligosaccharyl transferase complex. *J. Biol. Chem. 280*, 20261−20267.

(12) Jaffee, M. B., and Imperiali, B. (2011) Exploiting topological constraints to reveal buried sequence motifs in the membrane-bound N-linked oligosaccharyl transferases. *Biochemistry 50*, 7557−7567.

(13) Maita, N., Nyirenda, J., Igura, M., Kamishikiryo, J., and Kohda, D. (2010) Comparative structural biology of eubacterial and archaeal oligosaccharyltransferases. *J. Biol. Chem. 285*, 4941−4950.

(14) Lizak, C., Gerber, S., Numao, S., Aebi, M., and Locher, K. P. (2011) X-ray structure of a bacterial oligosaccharyltransferase. *Nature 474*, 350−355.

(15) Bause, E., and Legler, G. (1981) The role of the hydroxy amino acid in the triplet sequence Asn-Xaa-Thr(Ser) for the N-glycosylation step during glycoprotein biosynthesis. *Biochem. J. 195*, 639−644.

(16) Imperiali, B., Shannon, K. L., and Rickert, K. W. (1992) Role of peptide conformation in asparagine-linked glycosylation. *J. Am. Chem. Soc. 114*, 7942−7944.

(17) Otwinowski, Z., and Minor, W. (1997) Processing of X-ray Diffraction Data Collected in Oscillation Mode. *Methods Enzymol. 276*, 307−326.

(18) Vonrhein, C., Blanc, E., Roversi, P., and Bricogne, G. (2007) Automated structure solution with autoSHARP. *Methods Mol. Biol. 364*, 215−230.

(19) Langer, G., Cohen, S. X., Lamzin, V. S., and Perrakis, A. (2008) Automated macromolecular model building for X-ray crystallography using ARP/wARP version 7. *Nat. Protoc. 3*, 1171−1179.
(20) Emsley, P., and Cowtan, K. (2004) Coot: model-building tools for molecular graphics. *Acta Crystallogr., Sect. D: Biol. Crystallogr. 60*, 2126−2132.
(21) Brunger, A. T., Adams, P. D., Clore, G. M., DeLano, W. L., Gros, P., Grosse-Kunstleve, R. W., Jiang, J. S., Kuszewski, J., Nilges, M., Pannu, N. S., Read, R. J., Rice, L. M., Simonson, T., and Warren, G. L. (1998) Crystallography & NMR system: A new software suite for macromolecular structure determination. *Acta Crystallogr., Sect. D: Biol. Crystallogr. 54*, 905−921.
(22) Standley, D. M., Toh, H., and Nakamura, H. (2005) GASH: an improved algorithm for maximizing the number of equivalent residues between two protein structures. *BMC Bioinf. 6*, 221.
(23) Katoh, K., and Toh, H. (2008) Recent developments in the MAFFT multiple sequence alignment program. *Briefings Bioinf. 9*, 286−298.
(24) Igura, M., and Kohda, D. (2011) Selective control of oligosaccharide transfer efficiency for the N-glycosylation sequon by a point mutation in oligosaccharyltransferase. *J. Biol. Chem. 286*, 13255−13260.
(25) Ochman, H., Gerber, A. S., and Hartl, D. L. (1988) Genetic applications of an inverse polymerase chain reaction. *Genetics 120*, 621−623.
(26) Kohda, D., Yamada, M., Igura, M., Kamishikiryo, J., and Maenaka, K. (2007) New oligosaccharyltransferase assay method. *Glycobiology 17*, 1175−1182.
(27) Igura, M., and Kohda, D. (2011) Quantitative assessment of the preferences for the amino acid residues flanking archaeal N-linked glycosylation sites. *Glycobiology 21*, 575−583.
(28) Ben-Dor, S., Esterman, N., Rubin, E., and Sharon, N. (2004) Biases and complex patterns in the residues flanking protein N-glycosylation sites. *Glycobiology 14*, 95−101.
(29) Schwarz, F., and Aebi, M. (2011) Mechanisms and principles of N-linked protein glycosylation. *Curr. Opin. Struct. Biol. 21*, 576−582.
(30) Jarrell, K. F., Jones, G. M., and Nair, D. B. (2010) Biosynthesis and role of N-linked glycosylation in cell surface structures of archaea with a focus on flagella and s layers. *Int. J. Microbiol. 2010*, 470138.